




Structural, optical and Urbach energy properties of ITO/CdS and ITO/ZnO/CdS bi-layer thin films

M. Nagaraja^{1,*} , P. Raghu², H. M. Mahesh³, and Jayadev Pattar⁴

¹Department of Physics, SSIT, Sri Siddhartha Academy of Higher Education, Tumakuru 572107, India

²Department of Electronics, Govt. First Grade College Kuvempunagar, Mysore 570023, India

³Department of Electronic Science, Bangalore University, Bengaluru 560056, India

⁴School of Physics, REVA University, Bengaluru 560064, India

Received: 10 December 2020

Accepted: 16 February 2021

Published online:

3 March 2021

© The Author(s), under exclusive licence to Springer Science+Business Media, LLC part of Springer Nature 2021

ABSTRACT

The thin films of ITO/CdS and ITO/ZnO/CdS bi-layer have been fabricated and studied for structural, morphological, optical, and Urbach energy properties. ZnO thin films were coated onto ITO plated glass slides by a spin-coating method and CdS thin films by electron beam evaporation method. X-Ray Diffraction patterns of both ITO/CdS and ITO/ZnO/CdS thin films confirmed the hexagonal wurtzite structure of ZnO and hexagonal structure of CdS, respectively. AFM images show better uniformity and bigger grain size in the case of ITO/ZnO/CdS samples. Optical transmittance spectra show a slight redshift (~ 493 nm to ~ 505 nm) for the film ITO/ZnO/CdS compared to ITO/CdS. Urbach energy was calculated for all the samples to study the structural imperfections leading to the band tails. A decrease in Urbach energy is observed for ITO/ZnO/CdS compared to ITO/CdS. The obtained results indicate that the ITO/ZnO/CdS thin films are more suitable for optoelectronic devices compared to ITO/CdS films. The results obtained are discussed in detail and presented in this paper.

1 Introduction

Cadmium sulfide (CdS) is one of the promising compound semiconductors having a direct optical bandgap of 2.42 eV which belongs to the II-VI group. CdS being an n-type semiconductor acts as an appropriate window layer for CdTe-based solar cells [1]. CdS is also extensively used in multi-layered Cu(In, Ga)Se₂ solar cells [2]. Many researchers utilized different thin-film coating techniques to prepare

CdS thin films such as CVD [3], electrodeposition [4], pulsed direct current magnetron [5], and electron beam [6]. The properties of CdS layers can largely influence the performance of CdS/CdTe-based heterojunction solar cells [7]. However, thin films of CdS suffer from pin-holes and short in grain boundaries, and also CdS will diffuse into CdTe film during the fabrication of solar cells which leads to lateral junction in-homogeneity [8]. To overcome the limitations of CdS using bi-layer thin-film techniques,

Address correspondence to E-mail: madihally.nagaraja@gmail.com

Hernandez-Calderon et al. [9] reported the deposition and characterization of Cadmium Sulfide (CdS)/Zinc Sulfide (ZnS) bi-layers buffer configuration for thin-film solar cells. They have shown that, CdS/ZnS bi-layers buffer configurations as an effective alternative to the single CdS buffer layer. Xia et al. [10] developed a buffer layer based on Te/Cu bi-layer using the vapor deposition method. This buffer layer imparted useful information of ohmic contact to CdS/CdTe solar cells. Enhanced efficiency and stability were obtained by optimizing the Cu/Te compositions and the thermal activation conditions. Li et al. [11] studied the Copper Iodide (CuI) as a buffer layer CdS/CdTe solar cell. By optimizing the thickness of the CuI layer, they achieved a maximum efficiency of 14.5%. Also, they carried out the long time device stressing test and demonstrated the CdTe solar cells with a CuI buffer layer which has much better device stability compared to the solar cells with a Cu/Au bi-layer metal contact.

In this research work, the Zinc oxide (ZnO) layer is used to fabricate the ZnO/CdS bi-layer thin film. ZnO is selected to fabricate ZnO/CdS bi-layer because of its exciting properties such as wide direct bandgap, large exciton binding energy, high melting temperature, good chemical stability, inexpensive growth, non-toxicity, and its various electronic device applications [12]. In this research paper, we have reported the fabrication and characterization of the new ZnO/CdS bi-layer on ITO coated glass slides. On the surface of ITO coated glass plate, ZnO thin film is formed using a sol-gel spin-coating technique. Further, CdS is coated on ZnO using the e-beam evaporation method. To compare, the fabricated ITO/CdS and ITO/ZnO/CdS bi-layer thin films were characterized for structural properties using XRD morphology studies using AFM and optical properties by UV-Vis spectrophotometer.

2 Experimental

2.1 Thin-film coating

The ITO coated glass substrate was procured from Sigma-Aldrich (Sheet Resistance = $8 \Omega/\text{cm}^2$) and was used for the bi-layer deposition. On one set of glass slides, ZnO thin films were coated using a spin-coater Apex Instruments Co., Calcutta, Model NXG M1 with a speed of 3000 rpm for the 60 s. The thickness of

ZnO thin film was measured to be 300 nm by the spectroscopic ellipsometry method. The detailed preparation of ZnO thin films has been reported in Raghu et al. [13].

A layer of CdS was then coated on both sets of samples that are on ITO glass slides and ITO/ZnO layer by the e-beam evaporation method using vacuum coating unit Model 12A4D (Hind High Vacuum Company, Bangalore). The substrate temperature of 130 °C was maintained on the rotating substrate to get a uniform coating. The evaporation of CdS was made at the rate of 1 Å/sec and in situ thickness was measured to be nearly 300 nm using a thickness monitor fitted on the coating unit. After CdS coating, ITO/CdS and ITO/ZnO/CdS films were annealed at 450 °C for 1 h under a 10^{-5} torr vacuum. These samples were characterized by structural, morphological, and optical properties.

2.2 Instrumentation

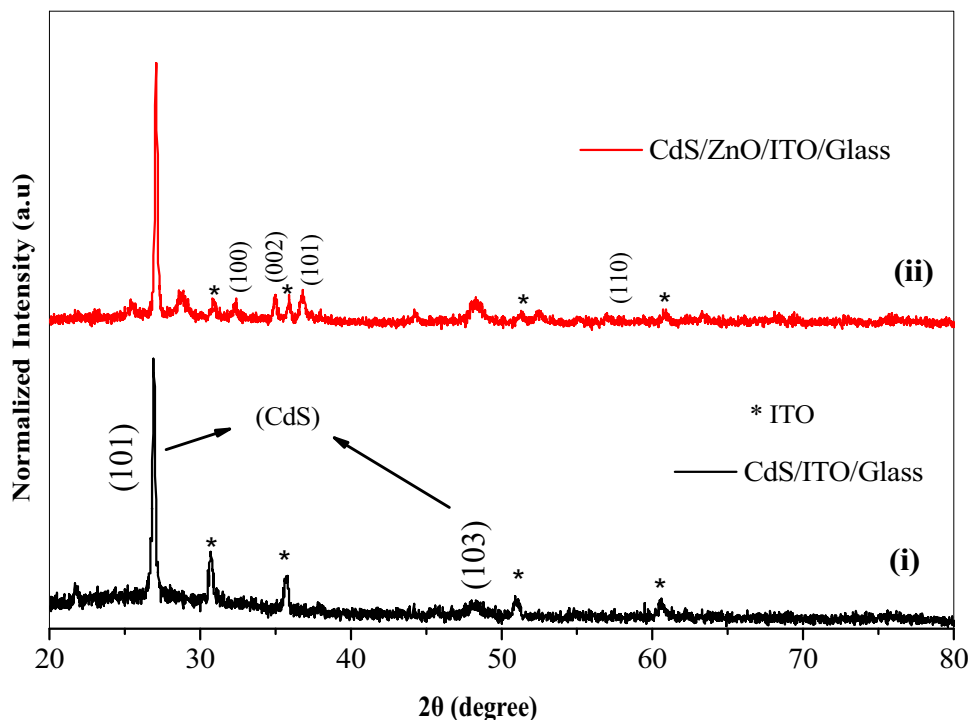
Structural properties of prepared samples were carried out using X-ray diffraction (XRD) spectra using Philips Xpert X-Ray diffractometer with monochromatic Cu-K α radiation ($\lambda = 1.54 \text{ \AA}$). Surface Morphology of bi-layer thin films was recorded using the APE Research instrument (model AFM A100) in non-contact mode. Optical properties were studied using UV-Vis Infrared Spectrophotometer (Ocean Optics, USB4000-XR USA).

3 Results and discussion

3.1 Structural properties

Figure 1i shows the XRD patterns of ITO/CdS thin-film coated glass substrate. The prominent peaks observed at 2θ values of 26.96° (101) and 48.28° (103) indicates the polycrystalline hexagonal structure of CdS and matches with JCPDS data JCPDS 41-1049 [14]. Figure 1ii depicts the XRD spectra of the ITO/ZnO/CdS bi-layer. The peaks at 2θ values 32.41, 34.9, and 36.89 are indexed to the hexagonal wurtzite structure of ZnO indexed to JCPDS (036-1451) [15] along with two prominent peaks of CdS. The remaining peaks observed in XRD as marked with a star are attributed to the ITO substrate as observed by other researchers with (JCPDS file No. 06-0416) [16]. The XRD of ITO/ZnO/CdS bi-layer shows peaks of

Fig. 1 XRD pattern of CdS/ITO/Glass and CdS/ZnO/ITO/Glass deposited thin films



ITO, ZnO as well as CdS because all these layers are very thin and X-rays have diffracted through the layers of thin films. The particle size of ITO/CdS and ITO/ZnO/CdS samples was estimated for CdS peaks using Scherrer's formula and found to be 38.76 nm and 42.66 nm, respectively. This indicates that the ITO/ZnO/CdS films have larger particles and improved crystallinity compared to ITO/CdS films. It seems that ZnO buffer layer helps CdS particles to agglomerate uniformly to form a continuous layer or reduces defects with enhanced crystallinity after annealing.

3.2 Morphology

The AFM micrographs of ITO/CdS and ITO/ZnO/CdS films were shown in Fig. 2a and b, respectively. A comparison between these two images immediately revealed the modification in their microstructure. The bi-layer thin-film structure, ITO/ZnO/CdS showed more uniform and larger grains of $\sim 0.5 \mu\text{m}$ (500 nm) in size indicating the improvement in the crystalline structure. The AFM parameters such as R_a and R_{rms} were found to increase (70.5 nm and 88.2 nm respectively) compared to ITO/CdS thin film (4.07 nm and 5.27 nm, respectively). The morphology results indicate the formation of uniform continuous bi-layer thin films. The larger and well-connected

grains of ITO/ZnO/CdS films may be due to proper growth of CdS onto the ZnO layer due to good adherence or reduction in the voids or defects.

3.3 Optical properties

The optimization of the ZnO thin-film layer is an important consideration for the fabrication of CdTe-based solar cell devices [17]. Therefore, ITO/CdS and ITO/ZnO/CdS bi-layers have been studied for optical transmittance properties using a UV-Vis spectrophotometer. The % transmittance of all thin-film layers is shown in Fig. 3. It is noticed that all these thin films have shown a sharp fall in transmittance at the particular band edge. This indicates good crystallinity and the direct bandgap nature of deposited films [18]. Further, the absorption edge of the bi-layer ITO/ZnO/CdS sample has shown a redshift comparing with ITO/CdS film ($\sim 493 \text{ nm}$ to $\sim 505 \text{ nm}$). However, single layer samples showed at $\sim 300 \text{ nm}$ and $\sim 370 \text{ nm}$ for ITO and ZnO thin films, respectively. The redshift in the bi-layer films is due to a change in the crystalline structure and morphology. A decrease in transmittance was also observed with the increased thickness of the sample. The films with the lower thickness (i.e., single layer) show high transmission, while the films of a higher thickness

Fig. 2 AFM images of **a** CdS/ITO/Glass and **b** CdS/ZnO/ITO/Glass

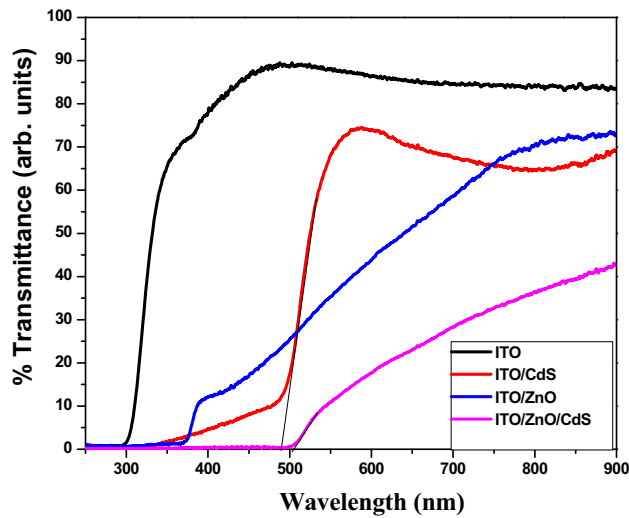
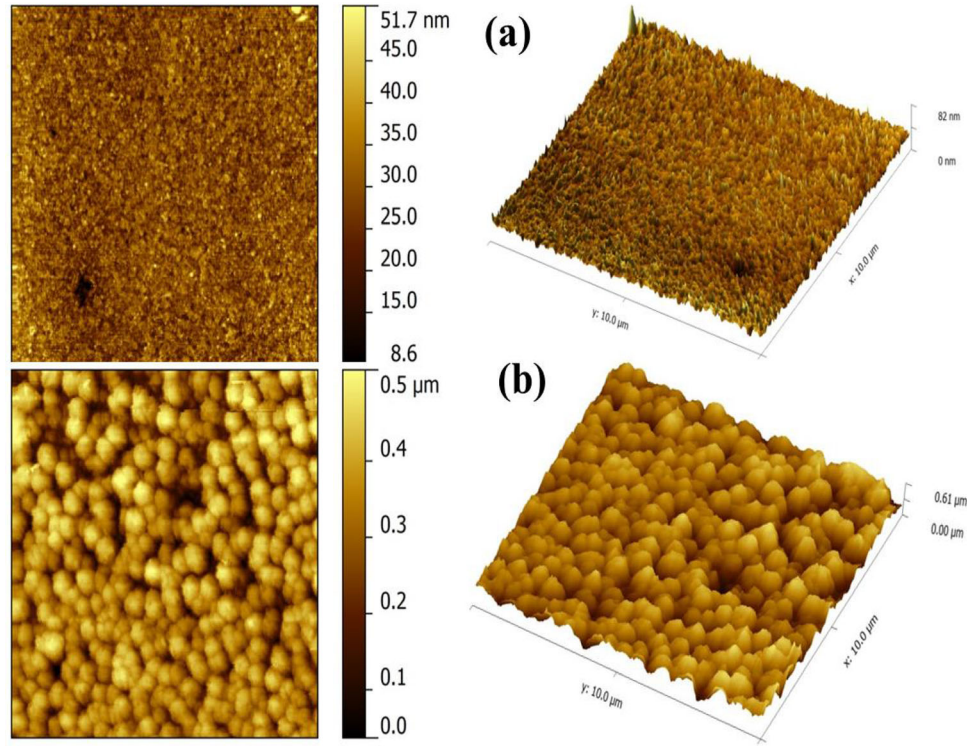


Fig. 3 Plot of transmittance spectra versus wavelength for a different layer of thin films

(i.e., bi-layer thin film) exhibit low transmission in the visible region.

The optical bandgap of all the deposited films was calculated using the Tauc formula for direct bandgap semiconductors [19],

$$(\alpha h\nu)^2 = A(h\nu - E_g) \tag{1}$$

Here α - absorption coefficient, A and h -constant values, E_g - optical bandgap energy, and ν - photon energy. The values of optical bandgap energy of the thin film are obtained by extrapolating the linear portion of the plot of $(\alpha h\nu)^2$ versus $h\nu$ to $\alpha = 0$. The curve indicates the straight-line fit over the higher energy range above the absorption edge which confirms the direct optical transition near the absorption edge. Figure 4 shows $(\alpha h\nu)^2$ versus $(E_g) h\nu$ curves of (a) ITO, (b) ITO/CdS, (c) ITO/ZnO and (d) ITO/ZnO/CdS thin films. The E_g of these films is listed in Table 1. Due to better morphology and crystal size, a slight increase in the energy gap has been observed in the ITO/ZnO/CdS sample than the ITO/CdS sample [20–23]. By inducing a layer of ZnO thin film between ITO and CdS can enhance the crystallinity and morphology with no considerable change in the optical energy gap.

3.4 Urbach energy

The change in the energy gap of bi-layer films may be due to improved morphology or reduced defects. To highlight the effect of defects on these films, an Urbach energy calculation has been carried out. The defects create an absorption tail in the absorption spectrum, which further extends into the forbidden

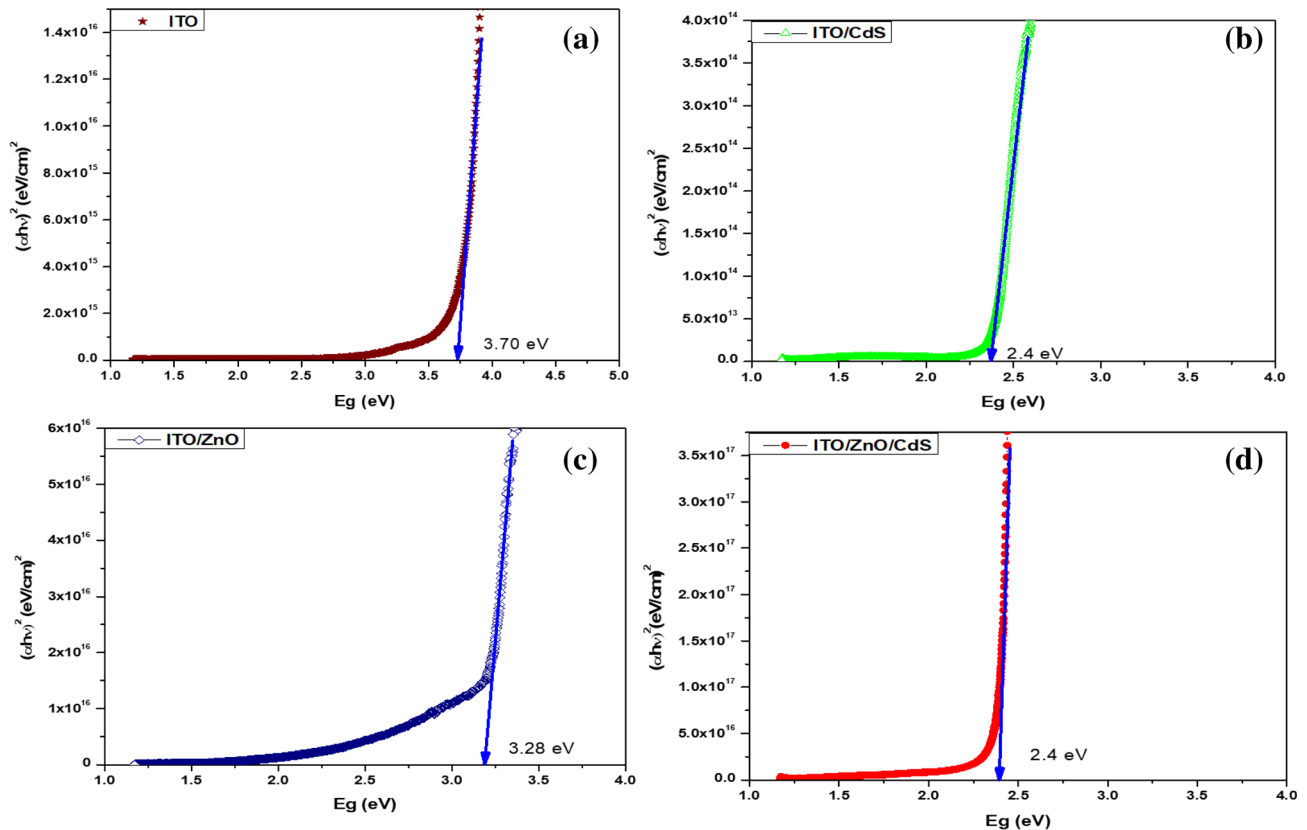


Fig. 4 Optical energy gap of **a** ITO, **b** ITO/CdS, **c** ITO/ZnO, **d** ITO/ZnO/CdS thin films

Table 1 Energy gap values of different thin films

Sample	Direct bandgap E_g (eV)	Urbach energy (meV)	Max. % transmittance
ITO	3.7	241	89.48
ITO/CdS	2.37	139	74.54
ITO/ZnO	3.28	139	76.51
ITO/ZnO/CdS	2.4	121	47.62

gap [24]. This absorption tail is called an Urbach tail and it is associated with the Urbach energy. Urbach energy is also associated with localized states of amorphous structure in amorphous materials. Polycrystalline materials also have Urbach energy in the forbidden gap due to the presence of disordered atoms in the amorphous phase. The expansion of energy bands reduces the optical bandwidth in the materials [25]. Usually, Urbach energy indicates the disorder of phonon states in the film. Urbach energy is governed by the structural disorder, an imperfection in stoichiometric and passivation at the surface [26]. At the bandgap energy, the generation of absorption edge is due to electron–phonon interaction or due to exciton–phonon interaction. The equation used to calculate Urbach energy is [27]

$$\alpha = \alpha_0 \exp \left[\frac{E - E_0}{E_U} \right] \quad (2)$$

where E_U is the Urbach energy which gives the width of the band tail. α_0 and E_0 are the Urbach bundle convergence point coordinates. The decrease in Urbach energy with an addition of thin-film layers is observed from Fig. 5 which indicates the reduction in the structural disorder of atoms and defects. In the case of ITO/ZnO/CdS thin film, the reduction of Urbach energy is because of crystallization improvement and a slight reduction in the energy gap.

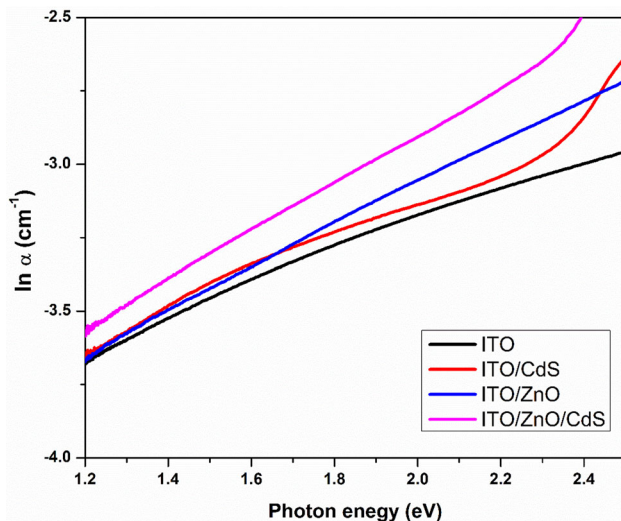


Fig. 5 Graphical representation of $(\text{Ln } \alpha)$ versus the photon energy ($h\nu$) of different thin-film samples to evaluate Urbach energy

4 Conclusions

This research paper reports the preparation of ITO/CdS and ITO/ZnO/CdS bi-layer thin films and their optical characteristics. The XRD results confirm the formation of a crystalline bi-layer with a wurtzite structure of ZnO and a hexagonal structure of CdS. The surface morphology using AFM confirms the continuous film with average grain sizes of around 500 nm for the ITO/ZnO/CdS. The optical bandgap for all the films was calculated to match with the reported literature. There is a slight decrease in the bandgap in ITO/ZnO/CdS film compared to ITO/CdS. Urbach energy values were calculated for all the samples and observed that with multilayer thin films disorders and charge traps can be avoided. These results suggest that the ITO/ZnO/CdS thin films have better crystallinity and morphology compared to ITO/CdS without much change in the optical properties. Hence, compared to ITO/CdS thin films, ITO/ZnO/CdS thin films are best suitable for optoelectronic device applications.

Funding

The authors declare that they have no known competing financial interests or personal relationships that could have appeared to influence the work reported in this paper. Also, we declare that “no

funds, grants, or other support was received” to carry out this work.

References

1. K.L. Chopra, P.D. Paulson, V. Dutta, *Prog. Photovolt.* (2004). <https://doi.org/10.1002/pip.541>
2. P. Jackson, D. Harisos, R. Wuerz, O. Kiowski, A. Bauer, T.M. Friedlmeier, M. Powalla, *Phys. Status Solidi RRL* (2014). <https://doi.org/10.1002/pssr.201409520>
3. Y. Sánchez, M. Espindola-rodríguez, H. Xie, S. López-marino, M. Neuschitzer, O. Vigil-galán, E. Saucedo, *Sol. Energy Mater. Sol. Cells* (2016). <https://doi.org/10.1016/j.solmat.2015.12.037>
4. M. Fathy, A.E.B. Kashyout, S. Elyamny, G.D. Roston, *Int. J. Electrochem. Sci.* **9**, 6155 (2014)
5. F. Lisco, P.M. Kaminski, A. Abbas, K. Bass, J.W. Bowers, G. Claudio, M. Losurdo, J.M. Walls, *Thin Solid Films* (2014). <https://doi.org/10.1016/j.tsf.2014.11.062>
6. R. Patel, N.C. Shivappa, S. Jeetendra, G. Sanjeev, M.S. Ilango, M.H. Matt, *Int. J. Mater. Sci. Appl.* (2014). <https://doi.org/10.11648/j.ijmsa.20140303.18>
7. K. Nakamura, M. Gotoh, T. Fujihara, T. Toyama, H. Okamoto, *Sol. Energy Mater. Sol. Cells* (2003). [https://doi.org/10.1016/S0927-0248\(02\)00154-X](https://doi.org/10.1016/S0927-0248(02)00154-X)
8. J. Han, C. Liao, T. Jiang, C. Spanheimer, G. Haindl, G. Fu, V. Krishnakumar, K. Zhao, A. Klein, W. Jaegermann, *J. Alloys Compd.* (2011). <https://doi.org/10.1016/j.jallcom.2010.12.085>
9. V. Hernández-Calderón, O. Vigil-Galán, F.A. Pulgarín-Agudelo, M. Courel, A. Arce-Plaza, F. Cruz-Gandarilla, F.J. Sánchez-Rodríguez, J. Roque-De la Puente, *Thin Solid Films* (2019). <https://doi.org/10.1016/j.tsf.2019.03.003>
10. W. Xia, H. Lin, H.N. Wu, C.W. Tang, I. Irfan, C. Wang, Y. Gao, Te/Cu bi-layer: a low-resistance back contact buffer for thin film CdS/CdTe solar cells. *Sol. Energy Mater. Sol. Cells* (2014). <https://doi.org/10.1016/j.solmat.2014.06.010>
11. X. Li, D. Xiao, L. Wu, D. Wang, G. Wang, D. Wang, *Sol. Energy* (2019). <https://doi.org/10.1016/j.solener.2019.04.082>
12. M. Norouzi, M. Kolahdouz, P. Ebrahimi, M. Ganjian, R. Soleimanzadeh, K. Narimani, H. Radamson, *Thin Solid Films* (2016). <https://doi.org/10.1016/j.tsf.2016.10.041>
13. P. Raghu, C.S. Naveen, J. Shailaja, H.M. Mahesh, *AIP Conf. Proc.* (2016). <https://doi.org/10.1063/1.4946520>
14. J. Planelles-Aragó, E. Cordocillo, R.A.S. Ferreira, L.D. Carlos, P. Escribano, *J. Mater. Chem.* (2011). <https://doi.org/10.1039/c0jm03188g>
15. A. Khorsand Zak, R. Razali, W.H. Abd Majid, M. Darroudi, Synthesis and characterization of a narrow size distribution of

- zinc oxide nanoparticles. *Int. J. Nanomed.* (2011). <https://doi.org/10.2147/ijn.s19693>
16. S. Luo, D. Yang, J. Feng, K.M. Ng, *J. Nanopart. Res.* (2014). <https://doi.org/10.1007/s11051-014-2561-5>
 17. M.A. Islam, Y. Sulaiman, N. Amin, *Chalcogenide Lett.* **8**, 65 (2011)
 18. C. Mao, W. Li, F. Wu, Y. Dou, L. Fang, H. Ruan, C. Kong, *J. Mater. Sci. Mater. Electron.* (2015). <https://doi.org/10.1007/s10854-015-3550-x>
 19. J. Tauc, A. Menth, *J. Non-Cryst. Sol.* (1972). [https://doi.org/10.1016/0022-3093\(72\)90194-9](https://doi.org/10.1016/0022-3093(72)90194-9)
 20. L. Xu, G. Zheng, J. Miao, F. Xian, *Appl. Surf. Sci.* (2012). <https://doi.org/10.1016/j.apsusc.2012.04.137>
 21. T. Liu, X. He, J. Zhang, L. Feng, L. Wu, W. Li, G. Zeng, B. Li, *J. Semicond.* (2012). <https://doi.org/10.1088/1674-4926/33/9/093003>
 22. G. Pérez-Hernández, J. Pantoja-Enríquez, B. Escobar-Morales, D. Martínez-Hernández, L.L. Díaz-Flores, C. Ricardez-Jiménez, N.R. Mathews, X. Mathew, *Thin Solid Films* (2013). <https://doi.org/10.1016/j.tsf.2012.11.092>
 23. H. Aydin, B. Gündüz, C. Aydin, *Synth. Met.* (2019). <https://doi.org/10.1016/j.synthmet.2019.04.002>
 24. B. Choudhury, A. Choudhury, *Phys. E* (2014). <https://doi.org/10.1016/j.physe.2013.10.014>
 25. A.S. Hassanien, A.A. Akl, *Phys. B* (2019). <https://doi.org/10.1016/j.physb.2019.411718>
 26. A. Mukherjee, M.R. Das, A. Banerjee, P. Mitra, *Thin Solid Films* (2020). <https://doi.org/10.1016/j.tsf.2020.138005>
 27. N. Ghobadi, P. Sohrabi, H. Reza Hatami, Correlation between the photocatalytic activity of CdSe nanostructured thin films with optical band gap and urbach energy. *Chem. Phys.* (2020). <https://doi.org/10.1016/j.chemphys.2020.110911>
- Publisher's Note** Springer Nature remains neutral with regard to jurisdictional claims in published maps and institutional affiliations.